Proceedings of CONF-MCEE 2027 Symposium: Advanced Nanomaterials and 2D Materials: Synthesis, Modeling, and Applications
DOI: 10.54254/2755-2721/2027.AD37748

# *Flexible Hydrogen-Bonded Organic Frameworks for Gas Adsorption-Separation: Stimuli-Responsive Mechanisms and Performance Tuning*

**Jionghao Wu**

*School of Chemical Engineering, East China University of Science and Technology, Shanghai, China*
*23010635@mail.ecust.edu.cn*

***Abstract.*** Industrial gas separation remains dominated by energy-intensive cryogenic distillation, stimulating research on adaptive porous adsorbents. Hydrogen-bonded organic frameworks (HOFs), self-assembled from organic units through reversible hydrogen bonds, are a distinctive class of crystalline porous materials whose intrinsic flexibility offers separation mechanisms unavailable to rigid metal-organic frameworks and covalent organic frameworks. Through literature analysis and comparative review of nine representative studies, this review examines the supramolecular origins of HOF flexibility, including neutral and charge-assisted hydrogen bonds, aromatic stacking and multi-force synergy, and categorizes dynamic behaviors into gate-opening and breathing, guest-induced pore expansion, reversible hydrogen-bond reconstruction and interpenetration-driven deformation. Design rules balancing flexibility and stability are distilled, and three benchmark systems, namely HOF-FJU-1 for ethylene/ethane fractionation, ZJU-HOF-8a for natural-gas purification and HOF-NKU-1 for humid sulfur-dioxide capture, are analyzed together with standardized evaluation methods. The analysis shows that controlled stimuli-responsive gating, rather than unrestricted flexibility, simultaneously delivers high uptake, selectivity and recyclability, and identifies molecular engineering, in situ characterization and computational screening as future priorities.

***Keywords:*** Hydrogen-bonded organic framework, Structural flexibility, Gas adsorption separation, Gate-opening effect

## 1. Introduction

Porous crystalline materials constitute a central platform for adsorption-based gas separation, and three principal families are distinguished by their linkage chemistry. Metal-organic frameworks (MOFs) use coordination bonds between metal nodes and organic linkers, and covalent organic frameworks (COFs) use covalent bonds between light elements; both families offer high and designable porosity but comparatively rigid backbones. Hydrogen-bonded organic frameworks (HOFs), by contrast, self-assemble from purely organic units through intermolecular hydrogen bonds and auxiliary weak interactions. Early HOFs frequently collapsed upon guest removal, and

© 2026 The Authors. This is an open access article distributed under the terms of the Creative Commons Attribution License 4.0 (https://creativecommons.org/licenses/by/4.0/).

DOI: 10.54254/2755-2721/2027.AD37748

only since permanent porosity was demonstrated in HOF-1 has rational framework design become possible [1, 2]. Their reversible linkages simultaneously create a stability challenge and an unusual structural adaptability unavailable to strong-bonded frameworks [3, 4].

Industrial purification tasks, including olefin/paraffin fractionation, natural-gas upgrading and flue-gas desulfurization, rely heavily on cryogenic distillation, which accounts for a substantial share of chemical-industry energy consumption. Adsorptive separation using stimuli-responsive adsorbents can lower this penalty, because an adaptive framework may remain closed to undesired components and open selectively toward a target gas, thereby transcending the conventional trade-off between uptake capacity and selectivity [5].

This review focuses specifically on flexible HOFs. Through literature analysis and comparative review of nine representative studies, their supramolecular driving forces and dynamic behaviors are first systematized; design strategies reconciling flexibility with stability are then summarized; representative gas separations and evaluation methods are examined; and remaining challenges are outlined, aiming to guide the rational design of energy-efficient HOF adsorbents and to inform subsequent research on dynamic porous molecular crystals.

## 2. Structural origins of flexibility in hydrogen-bonded organic frameworks

The flexibility of an HOF is not random motion but a controlled response encoded in the energy hierarchy of its supramolecular interactions and in the geometry of its building units.

### 2.1. Supramolecular driving forces for constructing flexible HOFs

#### 2.1.1. Hydrogen bonds and charge-assisted hydrogen bonds

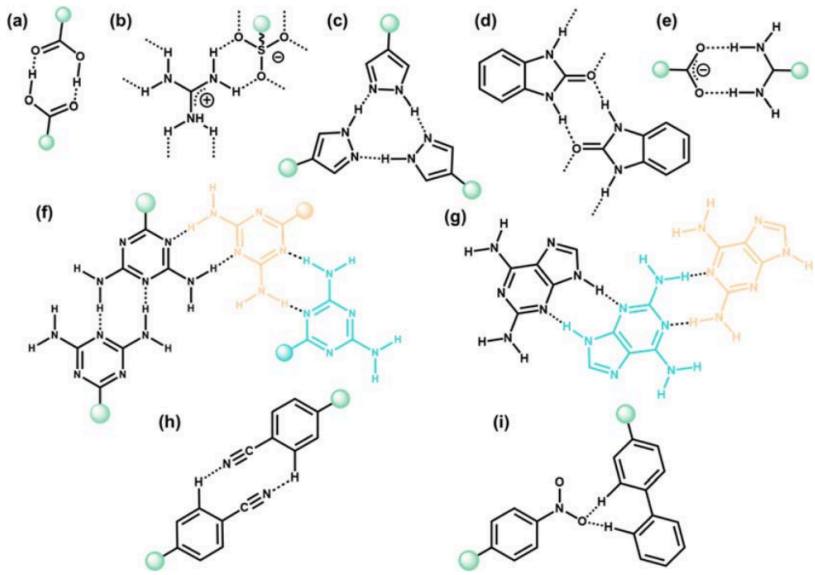



Figure 1. Representative supramolecular hydrogen-bonding synthons used for the construction of HOFs: (a) carboxyl dimer; (b) guanidinium-sulfonate; (c) pyrazole; (d) benzimidazolone; (e) amidinium-carboxylate; (f) 2,4-diaminotriazine; (g) 2,6-diaminopurine; (h) cyano group; (i) nitro group [5]

DOI: 10.54254/2755-2721/2027.AD37748

Hydrogen bonds constitute the primary linkage of HOFs, and the most widely used supramolecular synthons include carboxylic-acid dimers, 2,4-diaminotriazine, pyrazole, amidinium–carboxylate and guanidinium–sulfonate motifs, as summarized in Figure 1 [5]. Bond lengths of 2.5-3.2 Å, far exceeding the 1.2-1.5 Å of covalent bonds, and bond angles of 130°-180° that occasionally approach 90° leave geometrical room for local distortion. Bond energies of 10-40 kJ $mol^{-1}$ are likewise far below the 90-350 kJ $mol^{-1}$ of MOF coordination bonds and the 300-600 kJ $mol^{-1}$ of COF covalent bonds, explaining both the reversibility and the intrinsic softness of HOF networks [5]. Charge-assisted hydrogen bonds form between ionic partners such as ammonium–sulfonate, amidinium–carboxylate or guanidinium–sulfonate pairs, whose strength is reinforced by electrostatic attraction; such ionic HOFs gain improved thermal and chemical stability while retaining reversible, adaptive linkages, strengthening a lattice without making it rigid [6].

#### 2.1.2. Π–π aromatic stacking, van der Waals forces and multi-force synergistic effects

Hydrogen bonds define network topology, whereas secondary interactions determine how that topology deforms. Aromatic π–π stacking between conjugated tectons supplies cooperative cohesion that is decisive for layered HOFs; in the foundational HOF-1, diaminotriazine networks are further enforced by multiple stacking contacts that were essential to retaining permanent porosity after activation [2]. Complementary shape-fitted docking of planar conjugated cores enlarges the contact area as one of four reproducible stabilization strategies, while ubiquitous van der Waals and C–H···π interactions add a smooth, non-directional background energy [6]. Their synergy creates a hierarchical energy landscape in which hydrogen bonds repeatedly break and reform while stacking contacts act as soft hinges permitting reversible interlayer sliding [3, 5]. Planar, highly symmetric $C_3$-conjugated tectons combining rigid backbones with multiple hydrogen-bonding sites most reliably generate such robust-yet-flexible assemblies [3].

### 2.2. Typical dynamic-flexible behaviors of HOF frameworks

Depending on which interaction level is perturbed, flexible HOFs display four principal dynamic modes: pore-size and pore-shape changes, rearrangement of interpenetration or stacking, hydrogen-bond breakage and reconstruction, and local motion of structural subunits [5].

#### 2.2.1. Gate-opening gating effect and breathing transformation

The gate-opening effect denotes an abrupt pore opening once gas pressure reaches a guest-dependent threshold, observed most directly as a step in the adsorption isotherm, as shown in Figure 2. In HOF-1, carbon dioxide adsorption at 196 K remains limited below a relative pressure of 0.78 and then rises sharply with a large desorption hysteresis, signaling reversible transformation between the contracted guest-free HOF-1a and the expanded guest-loaded phase [2, 5]. Breathing refers to the corresponding reversible expansion and contraction of the unit cell. The threshold is itself stimulus dependent: in HOF-FJU-1, the gate-opening pressure for ethylene increases with temperature, allowing one framework to present different sieving windows under different operating conditions [7].

DOI: 10.54254/2755-2721/2027.AD37748

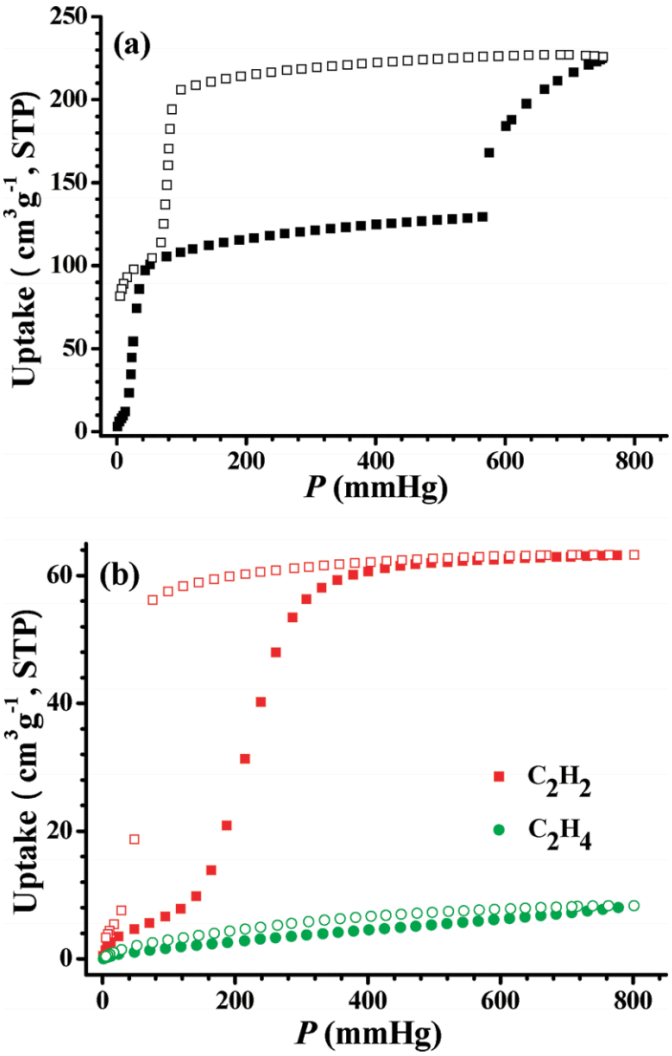



Figure 2. Gate-opening sorption of the foundational HOF-1: (a) $CO_2$ isotherm at 196 K showing a sharp uptake at $P/P_0 = 0.78$ with desorption hysteresis; (b) $C_2H_2$ and $C_2H_4$ isotherms at 273 K [2]

### 2.2.2. Guest-induced pore expansion and adaptive shape-memory behaviour

When guest–framework interactions are sufficiently strong, adsorption drives appreciable pore-volume expansion, as shown in Figure 3. The exceptionally adaptive 8PN framework, assembled from a tetrakis(nitrobiphenyl) ethane tecton, yields eight single-crystal phases whose pore volumes span 222.1–1816.0 Å³, interconverting reversibly under guest exchange, temperature variation and even mechanical pressure [5]. A milder counterpart is deformation without connectivity change: the one-dimensional channels of HOF-5 flatten from 22.5 × 34.7 Å² to 17.8 × 36.5 Å² on activation and the accessible volume falls from 55.3% to 41.1%, yet the original topology is retained [1, 5]. Such adaptive accommodation lets pore geometry match a target guest and relax again after desorption.

DOI: 10.54254/2755-2721/2027.AD37748

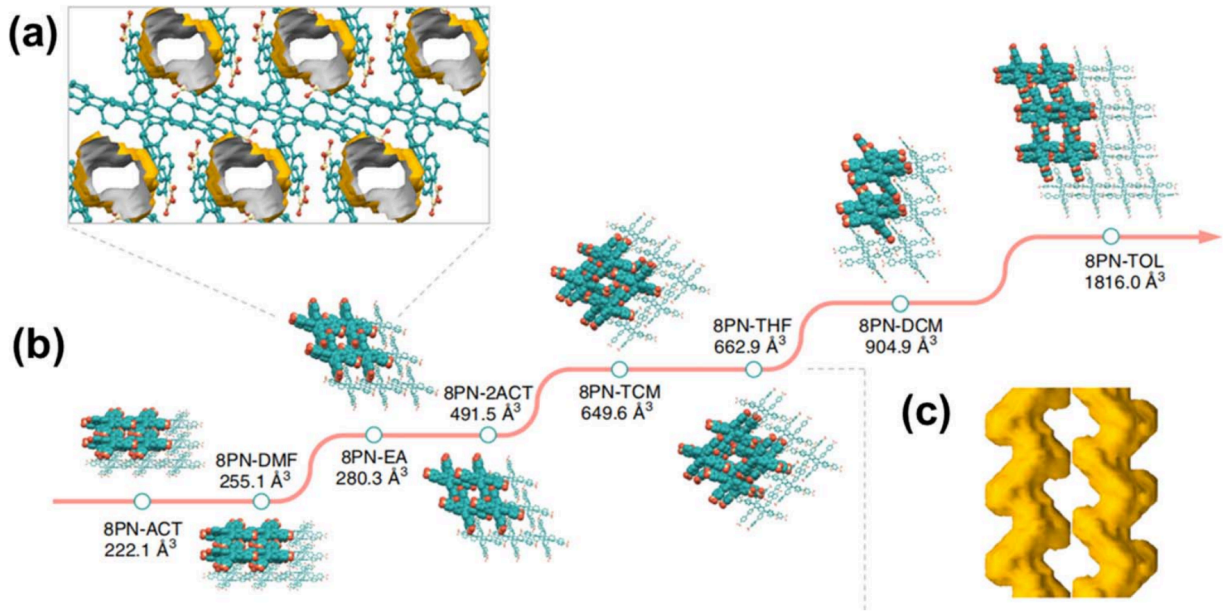



Figure 3. Eight crystalline phases of the adaptive 8PN framework: (a) Packing model of 8PN-EA in the [010] direction, with the solvent-accessible void space; (b) single-crystal X-ray structures of eight 8PN frameworks with varying void space; (c) S-shaped channel surface of 8PN-THF [5]

### 2.2.3. Reversible breakage–reconstruction of hydrogen-bond networks

The reversibility of hydrogen bonds permits an extreme form of self-healing dynamics. FDU-HOF-3 loses crystallinity upon ammonia adsorption because its carboxylic-acid dimers break and new carboxyl–ammonia acid–base interactions form; heating and degassing restore the initial network and crystallinity [5]. HOF-NBDA undergoes hydrogen-bond-pattern reorganization on activation from a monoclinic phase containing both carboxyl dimers and dimethylammonium charge-assisted bonds to an orthorhombic Fddd phase retaining only neutral dimers [5]. Reversible ethanol-bridged dimer transformations in HOF-30 further show that such reconstruction can cycle without cumulative damage [5].

### 2.2.4. Structural deformation from interpenetrated supramolecular entanglement

Interpenetration, in which several independent networks interweave, was traditionally treated as a rigidity-enhancing, pore-filling feature, but relative displacement of sub-networks also constitutes a distinct flexibility mechanism. HOF-FJU-1 contains a threefold-interpenetrated diamondoid network held by offset π–π contacts, and in situ diffraction detects slight expansion of its pore windows during gas loading [5, 7]. A more advanced case is ZJU-HOF-8, whose fourfold-interpenetrated lattice combines isolated catenane and infinite polycatenane motifs [3]; activation contracts its cell by 17.8%, and the entangled sub-networks slide apart only when a sufficiently adsorbable guest is present [8]. Interpenetration thus acts as a molecular spring coupling mechanical resilience with reversible, guest-gated motion.

DOI: 10.54254/2755-2721/2027.AD37748

### 2.3. Material-design strategies for balancing framework flexibility and structural stability

Permanent porosity and reversible dynamics impose opposing requirements, and four convergent design strategies emerge from the literature [5, 6]. First, rigid, highly conjugated and geometrically symmetric backbones carrying multiple hydrogen-bonding sites reduce uncontrolled floppiness while leaving local bond angles free to adjust, and planar $C_3$-symmetric carboxylic tectons are the most established realization [3, 6]. Second, the degree of interpenetration can be tuned through crystallization conditions, as shown by the twofold PETHOF-1 and fivefold PETHOF-2 isomers obtained from different solvent systems [4]. Third, charge-assisted hydrogen bonds raise linkage energy and therefore chemical and thermal robustness without eliminating reversibility [6]. Fourth, shape-fitted π–π stacking and additional C–H···π contacts collaboratively reinforce the skeleton, especially when combined with interpenetration [1, 6]. These principles convert the apparent weakness of noncovalent assembly into a designable combination of a stable backbone and locally responsive pores.

## 3. Representative applications of flexible HOFs in gas-mixture separation

The following case studies were selected because single-crystal structures, adsorption isotherms and dynamic-breakthrough evidence jointly establish how a specific flexible mechanism produces a measurable separation.

### 3.1. Separation of light-hydrocarbon mixtures

#### 3.1.1. Ethylene–ethane separation: flexible gating in HOF-FJU-1

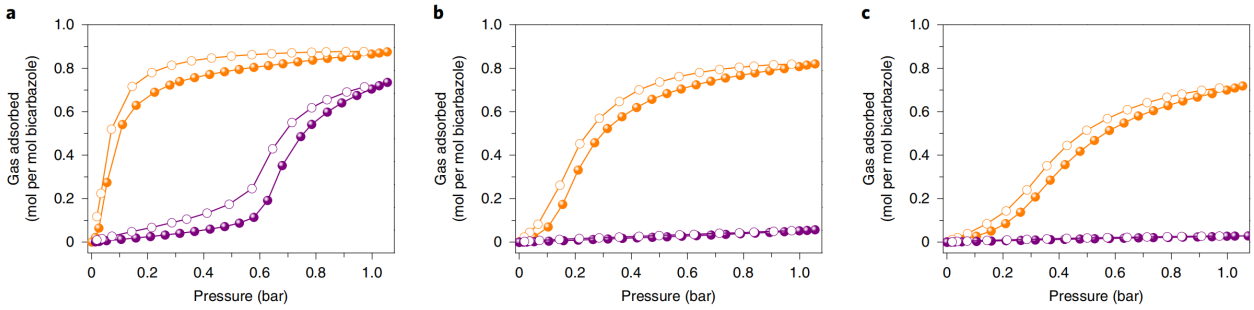



Figure 4. Temperature-dependent gating separation of $C_2H_4/C_2H_6$ in HOF-FJU-1a: (a-c) single-component isotherms at 298, 318 and 333 K [7]

Ethylene and ethane differ only marginally in kinetic dimensions, 3.28 × 4.18 × 4.84 versus 3.81 × 4.08 × 4.82 Å³, so static size exclusion is difficult. HOF-FJU-1 is assembled from 3,3′,6,6′-tetracyano-9,9′-bicarbazole through C–H···N hydrogen bonds into a threefold-interpenetrated diamondoid framework whose alternating cages and necks present pore windows of about 3.4 × 5.3 Å², as shown in Figure 4 [7]. At 298 K and 1 bar, activated HOF-FJU-1a takes up 47 cm³ g⁻¹ of ethylene, whereas ethane stays almost excluded below 0.58 bar and reaches only 38 cm³ g⁻¹ after its delayed gate opening; at 333 K, when the ethane threshold is raised, ethane uptake falls to 1 cm³ g⁻¹ while 36 cm³ g⁻¹ of ethylene is still adsorbed [7]. The ideal adsorbed solution theory (IAST) selectivity consequently rises from 10.5 at 298 K to 42.3 at 333 K, and fixed-bed breakthrough on equimolar feeds yields ethylene of 99.1% purity at 333 K [7]. Simulations confirm that neither gas

DOI: 10.54254/2755-2721/2027.AD37748

can enter a hypothetical rigid lattice, demonstrating that adsorption is enabled by framework motion itself [5, 7]. The material retains 97% of its captured-ethylene productivity over five cycles and survives solutions from pH 1 to 14, including concentrated hydrochloric acid and sodium hydroxide [7]. Earlier interpenetrated HOFs show complementary modes: sixfold-interpenetrated HOF-4a adsorbs 11.1 versus 3.6 $cm^3\ g^{-1}$ of ethylene and ethane (IAST selectivity 14), while ethane-selective HOF-76a delivers 7.2 L $kg^{-1}$ of pure ethylene during breakthrough [4].

### 3.1.2. Natural-gas purification: ZJU-HOF-8a with supramolecular entanglement

Natural-gas upgrading requires removing trace $C_2$+ hydrocarbons, especially propane and n-butane, from methane. ZJU-HOF-8a is built from 2,3,5,6-tetrakis(4-carboxyphenyl)pyrazine into a fourfold-interpenetrated diamondoid lattice in which catenane and polycatenane entanglement supported by weak C–H···N, C–H···O and C–H···π contacts generates robust 8.2 × 6.4 $Å^2$ channels ringed by 3.8 Å flexible pore pockets behind 2.4 Å windows, as shown in Figures 5 and 6 [8]. Activation contracts the unit-cell volume from 34353 to 28249 $Å^3$, a contraction of 17.8%. Methane and ethane bind too weakly to open the pockets, whereas n-butane and propane cross thresholds of 0.05 and 0.16 bar; at 296 K and 1 bar, uptakes reach 81.8 and 68.4 $cm^3\ g^{-1}$ for n-butane and propane against 56.3 and 11.3 $cm^3\ g^{-1}$ for ethane and methane [8]. IAST selectivities for 5:95 mixtures follow the same hierarchy, with n-butane/methane at 1059, propane/methane at 123 and ethane/methane at only 18 [8]. An n-butane-loaded crystal shows 13.5% framework expansion and pocket enlargement from 3.8 to 4.9 Å, directly visualizing guest-induced pocket opening [8]. Dynamic breakthrough gives retention times of 49, 181 and 262 min for ethane, propane and n-butane and a dynamic n-butane/methane selectivity of 136.5, maintained over five continuous cycles [8]. For comparison, permanently open HOF-TCBP with a Brunauer–Emmett–Teller (BET) area of 2066 $m^2\ g^{-1}$ reaches IAST $C_4$/methane selectivities of 147–241, placing the two design regimes as complementary rather than competing [4].

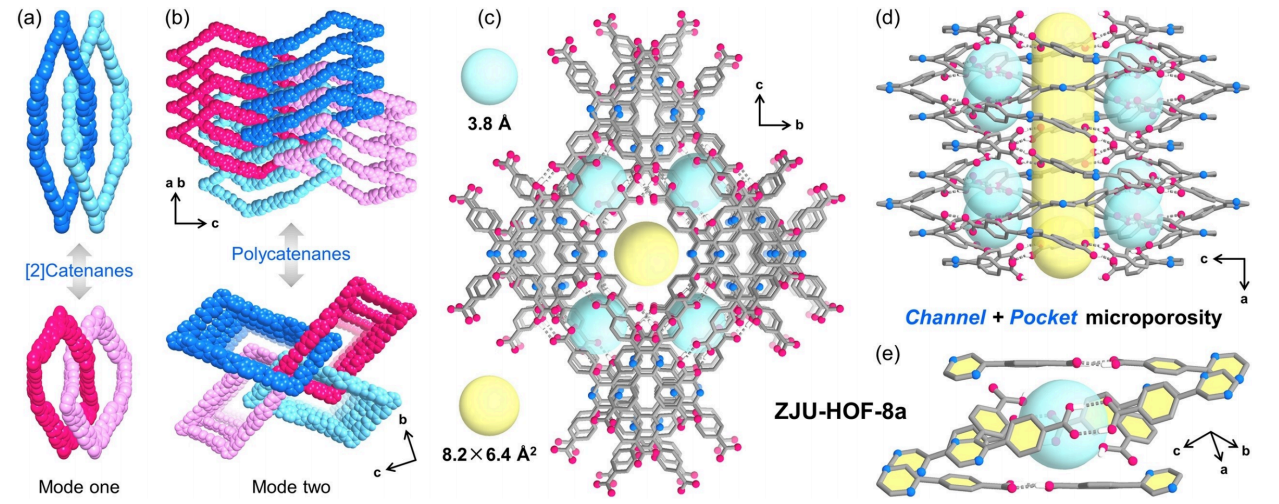



Figure 5. Supramolecular entanglement in ZJU-HOF-8a: isolated catenane and infinite polycatenane modes, rhombic pore channels and cage-like pore pockets [8]

DOI: 10.54254/2755-2721/2027.AD37748

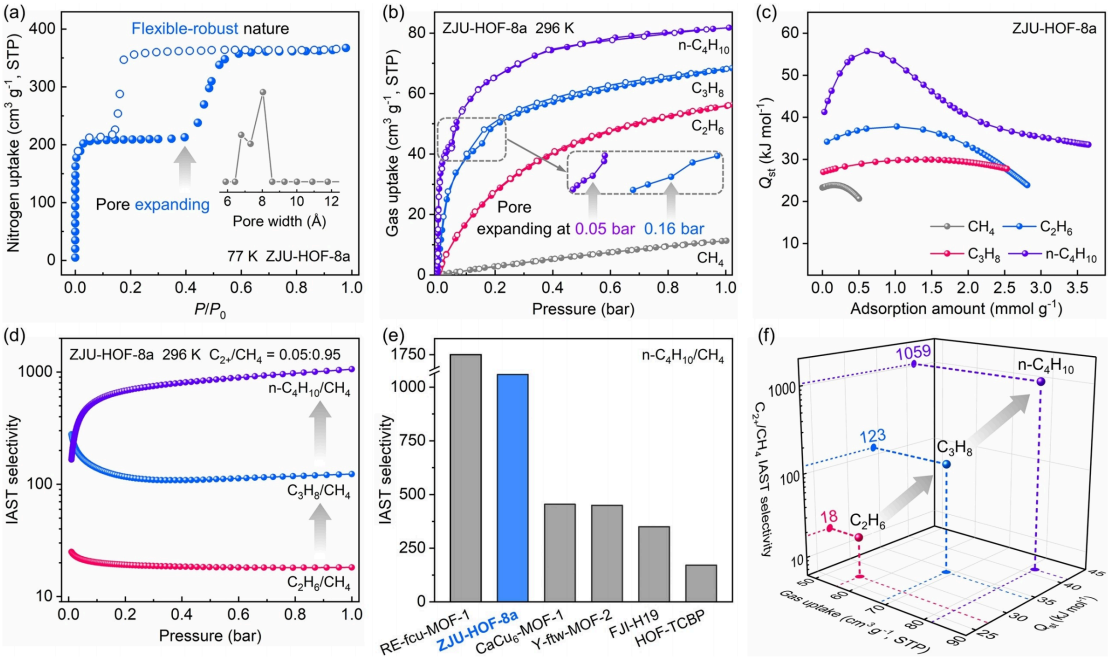



Figure 6. Flexible-robust sorption of ZJU-HOF-8a: (a) $N_2$ sorption isotherms of ZJU-HOF-8a at 77 K, with inset showing pore size distribution. (b) Gas sorption isotherms of ZJU-HOF-8a at 296 K, with inset showing partial pressures for pore expanding. (c) Isosteric heats of adsorption in ZJU-HOF-8a. (d) IAST selectivities ($C_2$+/$CH_4$, v/ v=0.05/0.95) of ZJU-HOF-8a at 296 K. (e) Comparison of n-$C_4H_{10}$/$CH_4$ IAST selectivity of ZJU-HOF-8a with several representative materials. (f) Overview of adsorbate-dependent gas sorption manners in ZJU-HOF-8a [8]

## 3.2. Acid-gas capture and selective separation

Acid-gas removal is dominated by sulfur-dioxide/carbon-dioxide separation, a counter-intuitive pair because sulfur dioxide with a kinetic diameter of 4.1 Å is larger than carbon dioxide at 3.3 Å yet more polarizable and strongly dipolar. HOF-NKU-1 is constructed from a chlorinated squaraine-derived tecton through C–O···H–C hydrogen bonds and π–π contacts into a threefold-interpenetrated square-lattice network with one-dimensional channels of 8.1 and 5.3 Å, as shown in Figure 7 [9]. Supercritical activation converts a nonporous closed phase into the open framework, and the combined shape-memory and guest-adaptive response keeps the pores open after the first cycle [9]. Sulfur dioxide is adsorbed steeply at low pressure, reaching 3.02 mmol $g^{-1}$ at only 0.01 bar and 6.74 mmol $g^{-1}$ (151 $cm^3$ $g^{-1}$) at 298 K and 1 bar, whereas carbon dioxide is limited to about 15 $cm^3$ $g^{-1}$; the IAST sulfur-dioxide/carbon-dioxide selectivity reaches 7331 for a 10:90 mixture [9]. Adsorption enthalpies of 50 versus 28 kJ $mol^{-1}$ and single-crystal structures showing dense sulfur-dioxide dimer packing and reversible cavity expansion from 6.887 × 8.238 to 9.159 × 6.779 $Å^2$ establish a guest-adaptive recognition mechanism [9]. Critically, the hydrophobic framework adsorbs only 17 mg $g^{-1}$ of water, and under 95% relative humidity, a simulated quaternary flue-gas mixture retains a dynamic sulfur-dioxide uptake of 1.62 mmol $g^{-1}$, only about 3% below dry conditions, over three humid cycles and after two weeks in 12 M acid or base [9]. Flexible HOFs can thus achieve reverse size-selective separation unavailable to rigid sieves without sacrificing humid stability.

DOI: 10.54254/2755-2721/2027.AD37748

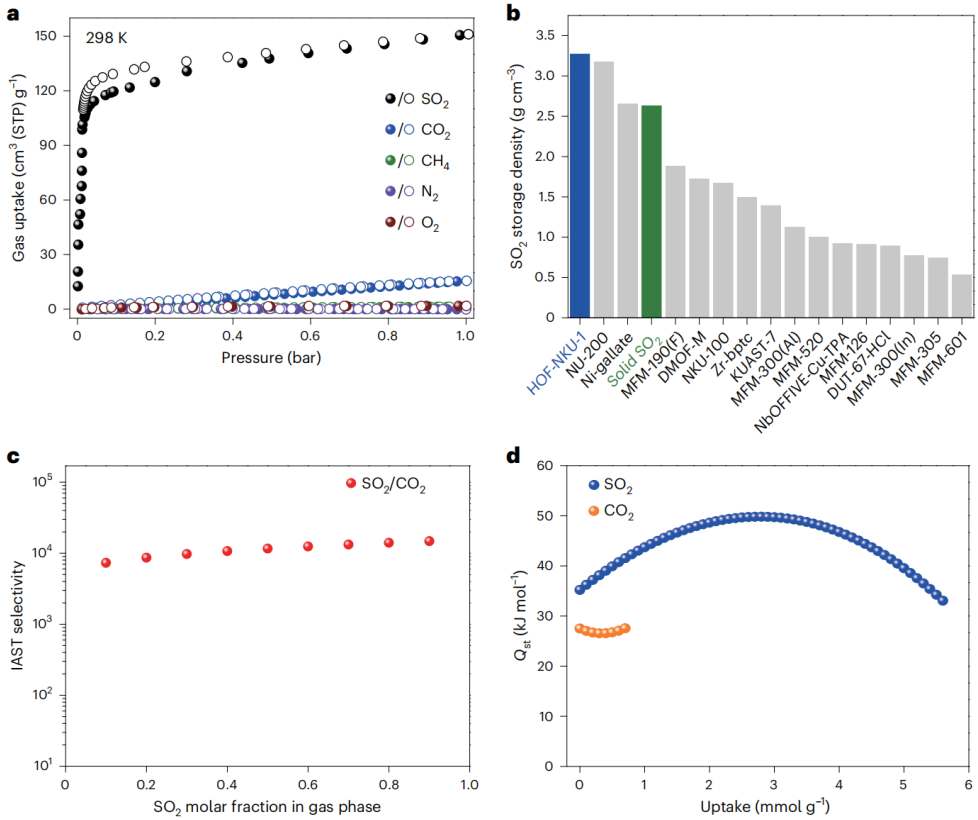



Figure 7. Gas sorption of HOF-NKU-1: single-component isotherms for $SO_2$, $CO_2$, $CH_4$, $N_2$ and $O_2$, together with the IAST $SO_2/CO_2$ selectivity of 7331. (a) Isotherms of $SO_2$, $CO_2$, $CH_4$, $N_2$ and $O_2$ at 298 K on HOF-NKU-1. The filled and open symbols represent adsorption and desorption, respectively. STP, standard temperature and pressure. (b) The comparison of $SO_2$ storage density in pores at ambient conditions (the porosity was estimated using Materials Studio 8.0 software with a probe radius of 1.4 Å). (c) IAST selectivity of $SO_2/CO_2$ on HOF-NKU-1 with varying molar fractions at 298 K and 1 bar. (d) The isosteric heat of absorption (Qst) for uptakes of $SO_2$ and $CO_2$ in HOF-NKU-1 [9]

## 3.3. Evaluation methods for separation performance of flexible HOF adsorbents

### 3.3.1. IAST-predicted selectivity

IAST converts single-component isotherms into binary-mixture selectivity and remains the standard first screening tool because mixture isotherms are experimentally demanding [4]. For flexible HOFs, however, calculations must span the full pressure range across the gate transition, since a stepped isotherm violates the assumption of a homogeneous adsorbed phase and selectivity can change several-fold at the threshold; the rise of HOF-FJU-1 selectivity from 10.5 to 42.3 with temperature and the order-of-magnitude enhancement of ZJU-HOF-8a after pocket opening illustrate this caveat [7, 8].

### 3.3.2. Dynamic breakthrough experiment and gate-threshold pressure measurement

Breakthrough experiments under continuous mixed flow record retention times, effluent purity and dynamic uptake under realistic conditions, and are indispensable because post-gating co-adsorption

DOI: 10.54254/2755-2721/2027.AD37748

cannot be predicted from single gases alone [7, 8]. The gate-threshold pressure should be located independently from the inflection of each isotherm and corroborated by in situ diffraction, which links the macroscopic step to a defined event such as window expansion or pocket opening [8, 9].

### 3.3.3. Adsorption–desorption cycling-stability assessment

Reversibility must be verified rather than assumed: repeated pressure-swing or temperature-swing cycles should be coupled with monitoring of uptake, breakthrough profile, crystallinity and surface area. The three benchmarks illustrate appropriate evidence levels, with HOF-FJU-1 retaining 97% capacity over five cycles, ZJU-HOF-8a maintaining n-butane/methane separation over five continuous cycles and HOF-NKU-1 preserving humid breakthrough over three cycles [7-9]. Recrystallization-based healing offers an additional regeneration route unique to hydrogen-bonded networks [1, 5].

## 4. Conclusion

This review examined flexible hydrogen-bonded organic frameworks as stimuli-responsive adsorbents for gas-mixture separation, integrating evidence from nine primary and review studies. Analysis of the supramolecular interactions shows that framework dynamics arise from the reversible hierarchy of neutral or charge-assisted hydrogen bonds, aromatic stacking and van der Waals contacts, which manifests as gate-opening and breathing, guest-adaptive expansion, hydrogen-bond reconstruction or interpenetration displacement. The three benchmark systems establish a consistent structure–performance relationship: controlled, guest-gated motion combined with a permanently robust backbone simultaneously achieves high capacity, exceptional selectivity and recyclability, as shown by temperature-tunable ethylene/ethane gating, entanglement-controlled natural-gas purification and reverse-selective humid sulfur-dioxide capture. The principal limitation of this review lies in its restricted set of case systems and membrane formats; large-scale synthesis and techno-economic assessment remain outside its scope. Future work should prioritize in situ structural characterization of transition states, predictive computational screening of gate-opening pressures, and translation of flexible HOFs into robust mixed-matrix membranes and shaped adsorbents for industrial service.

## References

[1] Lin, R. B., He, Y., Li, P., Wang, H., Zhou, W., & Chen, B. (2019). Multifunctional porous hydrogen-bonded organic framework materials. *Chemical Society Reviews, 48*(5), 1362-1389.

[2] He, Y., Xiang, S., & Chen, B. (2011). A microporous hydrogen-bonded organic framework for highly selective C2H2/C2H4 separation at ambient temperature. *Journal of the American Chemical Society, 133*(37), 14570-14573.

[3] Hisaki, I., Xin, C., Takahashi, K., & Nakamura, T. (2019). Designing hydrogen-bonded organic frameworks (HOFs) with permanent porosity. *Angewandte Chemie International Edition, 58*(33), 11160-11170.

[4] Wang, B., Lin, R. B., Zhang, Z., Xiang, S., & Chen, B. (2020). Hydrogen-bonded organic frameworks as a tunable platform for functional materials. *Journal of the American Chemical Society, 142*(34), 14399-14416.

[5] Li, J., & Chen, B. (2024). Flexible hydrogen-bonded organic frameworks (HOFs): Opportunities and challenges. *Chemical Science, 15*(26), 9874-9892.

[6] Song, X., Wang, Y., Wang, C., Wang, D., Zhuang, G., Kirlikovali, K. O., ... & Farha, O. K. (2022). Design rules of hydrogen-bonded organic frameworks with high chemical and thermal stabilities. *Journal of the American Chemical Society, 144*(24), 10663-10687.

[7] Yang, Y., Li, L., Lin, R. B., Ye, Y., Yao, Z., Yang, L., ... & Chen, B. (2021). Ethylene/ethane separation in a stable hydrogen-bonded organic framework through a gating mechanism. *Nature Chemistry, 13*(10), 933-939.

DOI: 10.54254/2755-2721/2027.AD37748

[8] Jiang, C., Wang, J. X., Liu, D., Wu, E., Gu, X. W., Zhang, X., ... & Qian, G. (2024). Supramolecular entanglement in a hydrogen-bonded organic framework enables flexible-robust porosity for highly efficient purification of natural gas. *Angewandte Chemie, 136*(26), e202404734.

[9] Li, L., Zhang, X., Lian, X., Zhang, L., Zhang, Z., Liu, X., ... & Bu, X. H. (2025). Flue gas desulfurization and SO2 recovery within a flexible hydrogen-bonded organic framework. *Nature Chemistry, 17*(5), 727-733.